Andesitic pyroclastic rocks injected laterally into weak lacustrine sediments within a Mesoproterozoic arc sequence, SW Namibia

Sierra C. Ohrmundt[1], Richard E. Hanson[1], and Virginia P. Andrews[1]

[1]School of Geology, Energy and the Environment, Texas Christian University, Fort Worth, TX 76129
(r.hanson@tcu.edu)

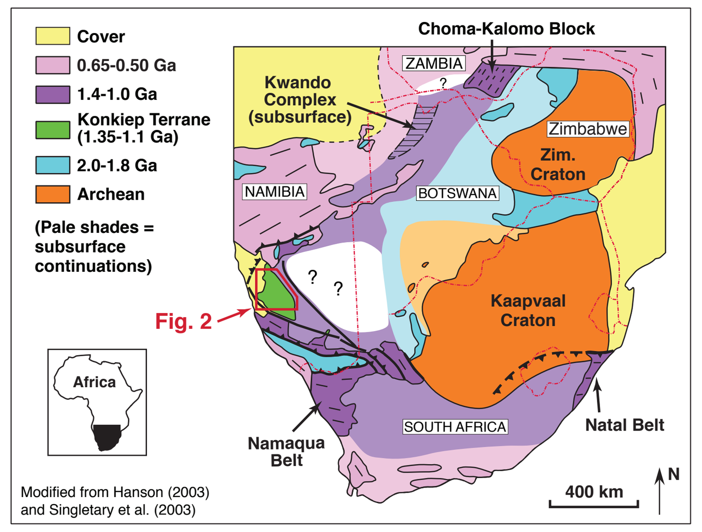

Fig. 1. Location of the Konkiep terrane within the Precambrian tectonic framework of southern Africa.

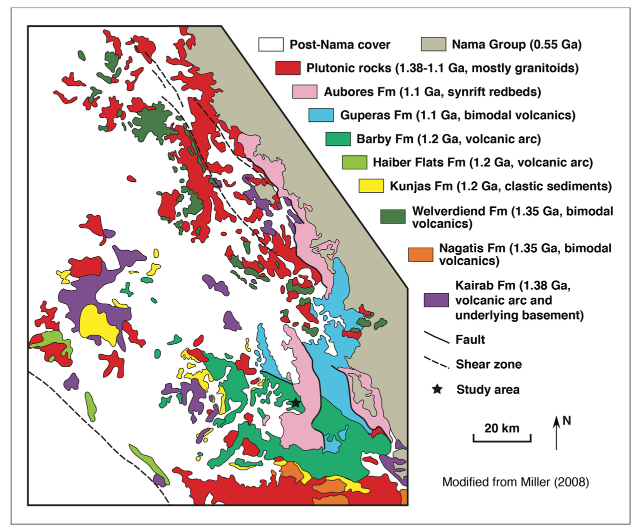

Fig. 2. Geological map of the main part of the Konkiep terrane (2008), showing location of study area.

Abstract

The 1.2 Ga volcanic arc rocks in the Barby Formation are well exposed in desert terrain in SW Namibia - this formation records the establishment of a major continental margin arc following earlier accretionary events. Recent field work has shown that large portions of the formation consist of pyroclastic fall deposits erupted from small volcanoes (fissures and scoria or spatter cones) in a region with poor drainage and abundant lakes.

Detailed mapping of a well-exposed section of the Barby Formation provides an oblique cross-sectional view of a succession of andesitic pyroclastic fall units intercalated with planar bedded lacustrine sediments as well as associated hypabyssal intrusions. Massively bedded units up to ~80 m thick show abundant bombs up to 60 cm across in a matrix of fluidal to angular lapilli, indicating deposition close to source vents undergoing primarily Strombolian-type eruptions. Hypabyssal dikes and sills are common, often cutting through the massively bedded pyroclastic units.

Also present are pyroclastic deposits that intrude lacustrine sedimentary packages at 12 locations spread out over a horizontal distance of ~600 m and a vertical stratigraphic sequence of ~300 m. These deposits contain similar bombs and lapilli as the pyroclastic fall deposits, but show clear fluidal intrusive relations with adjacent sedimentary units. In most cases, zones of peperite are formed in between the pyroclastic intrusions and the lacustrine sediments, consisting of fluidal bodies of vesicular basaltic andesite mingled with fine-grained sediment with preserved lamination. We infer that jets of intrusive pyroclastic material were blasted laterally into weak, unlithified lake sediments from one or more vent conduits feeding explosive eruptions at the surface; these jets are likely to have been forced out by collapse of the conduit inward. Fluidization of the sediment would have occurred as pore water was converted to steam, which would have facilitated lateral motion of the pyroclastic jets.

Geologic Framework

Mesoproterozoic arc rocks in SW Namibia occur within the Konkiep terrane (Fig. 1), which is a major tectonic element within the 1.4-1.0 Ga Namaqua-Natal orogenic belt that represents one of the main convergent margins active during assembly of the Rodinia supercontinent (Hanson, 2003; Jacobs et al., 2008; Miller, 2012). The Konkiep terrane contains a series of volcanic and sedimentary units and associated, dominantly granitoid plutonic rocks separated partly by major unconformities (Fig. 2; Watters, 1974; Miller, 2008). Metamorphic grade is typically in the zeolite and prehnite-pumpellyite facies. The timing of the different magmatic events recorded in the terrane is constrained primarily by U-Pb zircon crystallization ages (Miller, 2008; Cornell et al., 2015, 2016; Panzik et al., 2016). These data show that island-arc tholeiitic rocks of the ~1.38 Ga Kairab Formation represent the earliest arc magmatism in the terrane. Following accretion of this arc and its underlying metamorphic basement, renewed magmatism at ~1.35 Ga formed the bimodal (basaltic and rhyolitic) Nagatis and Welverdiend Formations, probably in rift environments. Development of a new continental margin arc is recorded by the ~1.2 Ga calc-alkaline Haiber Flats Formation and the calc-alkaline to shoshonitic Barby Formation, which is located farther inboard (Watters, 1974; Brown and Wilson, 1986; Hoal, 1990; Miller, 2012). These rocks are unconformably overlain by 1.1 Ga synrift bimodal rocks of the Guperas Formation and slightly younger redbeds of the Aubures Formation (Miller, 2008; Panzik et al., 2016).

The Barby Formation, which is the focus of the present work, contains a composite volcanic arc stratigraphic succession as much as 8 km thick. Our recent mapping in two well-exposed areas (Fig. 2) has revealed that significant parts of the formation consist of Hawaiian, Strombolian and phreatomagmatic pyroclastic deposits that were emplaced close to source vents (fissures or scoria and spatter cones) and are intercalated with fine-grained lacustrine strata, which are ubiquitous throughout the study area. The facies relations are consistent with the interpretation that these rocks accumulated in extensional basins during oblique subduction along the convergent margin (Hoal, 1993). At least in the limited areas we have so far investigated, there is no evidence for high-standing stratovolcanoes.

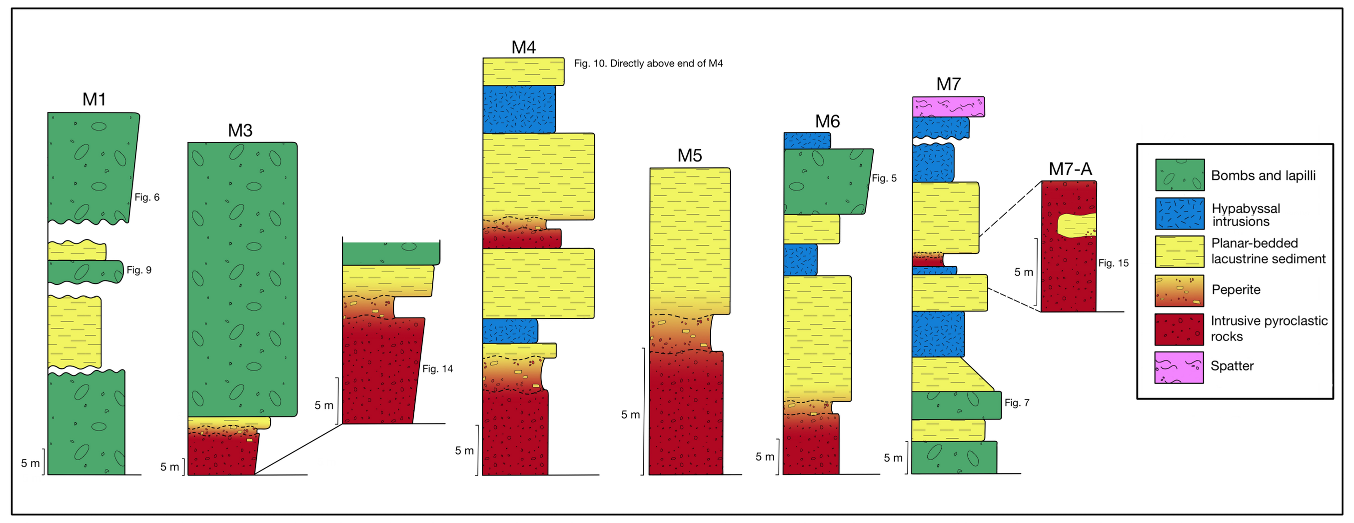

Fig. 4. Representative measured sections; locations are shown in Fig. 3. M7-A shows a discordant mass of intrusive pyroclastic rock cutting out part of the sequence shown in M7.

Study Area

The study area for this poster is located on the western margin of a half-graben occupied by Aubures redbeds (Fig. 2). Figure 3 is an oblique view of most of the study area and illustrates the main extrusive and intrusive lithofacies present, discussed below. Figure 4 shows representative measured sections of some of the units. The various units contain similar phenocryst populations (augite and altered olivine), suggesting they are closely linked petrogenetically. Based on petrographic comparisons with samples from other parts of the Barby Formation for which we have geochemical analyses (Andrews and Hanson, unpubl. data), we infer that the extrusive and intrusive rocks in the present study area are basaltic andesite to shoshonite in composition; geochemical studies of these rocks are in progress.

Lacustrine Deposits

The main extrusive pyroclastic deposits in the study area are separated by sequences up to 20 m thick of dominantly planar-bedded andesitic volcaniclastic mudstone, siltstone, sandstone and granule conglomerate (Figs. 4 and 5) inferred to have been deposited by sediment gravity flows and suspension sedimentation in lacustrine settings. Delicate planar lamination is characteristic of the finer grained clastic rocks, and coarser debris-flow deposits and turbidites typically form tabular units that are laterally continuous on the scale of individual outcrops.

Pyroclastic Deposits

The most impressive pyroclastic deposits are cliff-forming, poorly sorted, bomb-rich units as much as 80 m thick with little evidence of internal layering (Figs. 6 and 7). These units contain variable amounts of fluidal, elongate to ellipsoidal bombs ≤ 60 cm across, in which vesicularity ranges from 10 to 50 %, based on visual estimates. Juvenile angular lithic clasts (Fig. 8) and pieces of spatter (Fig. 9) occur in smaller amounts. Bomb sags are well developed where the bomb-rich deposits rest directly on lacustrine beds (Fig. 10). Agglomerate is present locally where the bombs are closely packed, but the bombs are generally dispersed within a matrix consisting dominantly of lapillistone (Figs. 7 and 8). Individual lapilli most commonly have fluidal outlines with ovoid, droplet-like, or somewhat elongate shapes and show the same range in vesicularity as the bombs (Fig. 8). Beds of coalesced spatter also occur (Fig. 4, measured section 7). The characteristics of the pyroclasts overall indicate derivation from explosive eruptions showing transitional Strombolian to Hawaiian behavior.

The lapillistone in some cases grades into meter-scale pockets of lapilli tuff that contain angular, blocky, poorly vesicular ash- and lapilli-sized particles (Fig. 11). In some cases, partly disaggregated pieces of sand and mud ≤ 60 cm long also occur within the lapilli tuff. We interpret the lapilli tuff to record a phreatomagmatic component in some of the eruptions, in which pyroclastic disruption of the magma was driven by release of magmatic volatiles coupled with explosive interactions between magma and water-rich lake sediment. Flashing of pore-water to steam in the sediments increased the energy of the eruptions and caused fine-scale explosive shattering of the magma (Wohletz, 1986).

Fig. 5. Interval of bedded lacustrine strata shown in measured section M-6 (Fig. 4); beds are overlain by cliff-forming bomb-rich unit.

Fig. 7. Basaltic andesite bombs in lapillistone matrix (M-7-3 in Fig. 4).

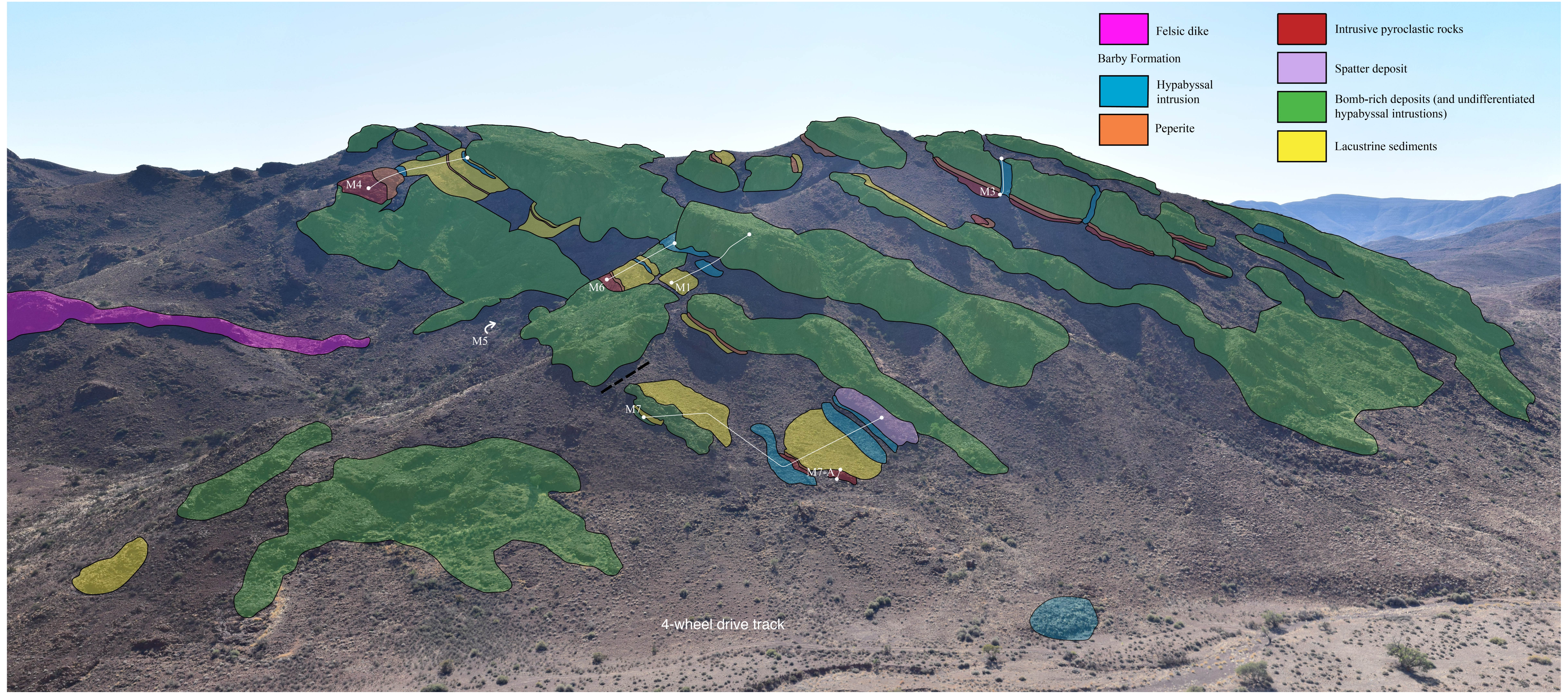

Fig. 3. Oblique cross sectional view of the study area, looking east. Locations of measured sections in Fig. 4 are indicated.

Fig. 8. Lapillistone matrix in bomb-rich unit. Note angular juvenile lithic block in lower left.

Fig. 10. Bomb sag (bomb outlined in red) at base of massive bomb-rich unit overlying lacustrine strata.

Fig. 11. Angular, poorly vesicular lapilli within a pocket of lapilli tuff that grades into more common lapillistone matrix (not visible in this view) in a bomb-rich unit.

Fig. 6. Massively bedded bomb-rich unit (M-1-6 in Fig. 4).

Fig. 9. Vesicular spatter within unit M-1-4 (Fig. 4). Blocky green crystals are altered augite phenocrysts.

Intrusive Pyroclastic Rocks

We have found pyroclastic rocks that show clear intrusive relations with lacustrine strata at 12 separate locations within the study area over a lateral distance of ~600 m and a vertical stratigraphic distance of ~300 m. The intrusive pyroclastic rocks form massive bodies ≥ 12 m across (Fig. 12), but their full dimensions are generally unclear because their margins are partly covered. They transgress bedding in the lacustrine sediments (Fig. 13), and in one case form a 1-m-dike injected into the host sediments. Tabular masses of sandstone up to 3 m long are enclosed within the pyroclastic material (Fig. 4 -- M7A) and show partly disrupted bedding and mixing along their margins with the adjacent pyroclasts. The intrusive pyroclastic rocks contain the same types of bombs dispersed in lapillistone or lapilli tuff as seen in the extrusive pyroclastic deposits (Figs. 12, 14, and 15). The bombs tend to be smaller (≤ 20 cm) than in the extrusive deposits, but otherwise the pyroclasts in the intrusive and extrusive units are indistinguishable. An intrusive origin is only obvious when the contacts of these pyroclastic masses with the host sedimentary strata are exposed.

Peperite

In most cases, zones of peperite up to 10 m thick separate the intrusive pyroclastic rocks from the adjacent sedimentary strata (Figs. 4 and 16) and show discordant contacts against relatively undisturbed bedded lacustrine deposits (Figs. 16 and 17). The peperite consists of fluidal clasts of basaltic andesite ≤ 50 cm across that contain 30-40 % vesicles and are surrounded by partly disrupted sandstone, siltstone and mudstone, in which planar lamination is preserved to various degrees (Fig. 18).

Fig. 12. Coherent basaltic andesite dike showing undulatory chilled margin against intrusive pyroclastic rock to right.

Fig. 13. Intrusive pyroclastic rock cutting sandstone and granule conglomerate.

Fig. 14. Elongate to ellipsoidal fluidal pyroclasts within intrusive pyroclastic rock (unit M-3-1 in Fig. 4).

Fig. 15. Intrusive pyroclastic rocks from M7-A.

Fig. 16. Large mass of peperite intruding bedded sediment (S) beneath a massive, bomb-rich unit. Fluidal basaltic andesite clasts in peperite weather more readily than the sediment host (examples are labeled “ba”). Arrow points to truncation of bedding in overlying sediment against discordant contact with peperite.

Fig. 17. Closer view of area indicated by arrow in Fig. 16.

Coherent Hypabyssal Intrusions

Coherent intrusions of poorly to nonvesicular basaltic andesite are common throughout the study area. They consist of dikes ≤ 10 m wide, sills ≤ 7 m thick and discordant intrusions with more irregular shapes as much as 50 m across. The dikes typically have planar chilled margins where they crosscut cliff-forming, bomb-rich units, but these margins become undulatory where the dikes intrude lacustrine strata, intrusive pyroclastic rocks and peperite (Fig. 12). In places, elongate, branching intrusive tongues up to several meters long extend from dikes or irregular intrusions into the adjacent units. Some of the tongues show partial disaggregation where they penetrated pyroclastic material (Fig. 19).

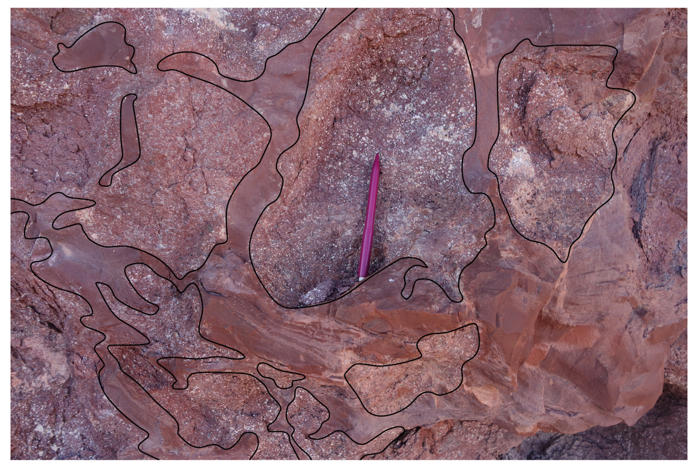

Fig. 18. View of peperite from a different area, showing fluidal bodies of vesicular basaltic andesite (outlined) separated by disrupted sediment that partly preserves planar lamination.

Fig. 19. Partly disaggregated intrusive tongue (outlined) penetrating extrusive pyroclastic deposits.

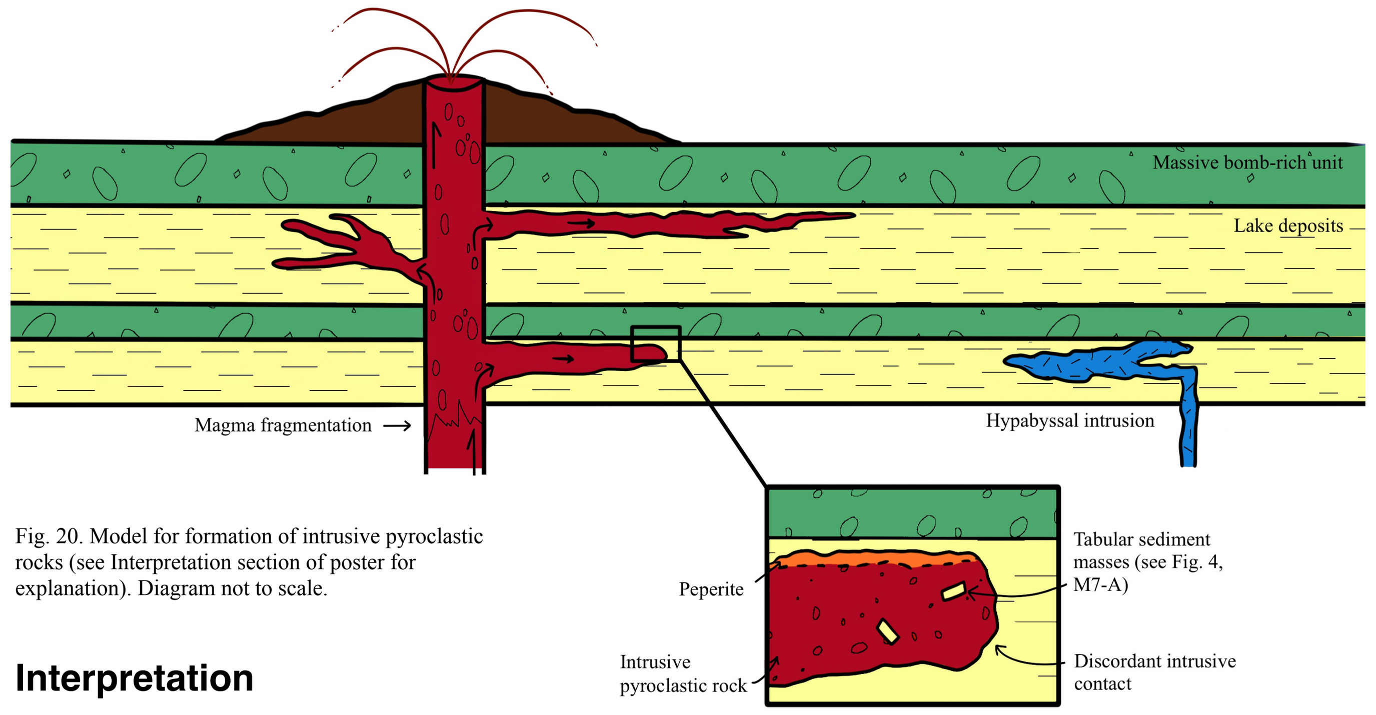

Fig. 20. Model for formation of intrusive pyroclastic rocks (see Interpretation section of poster for explanation). Diagram not to scale.

Interpretation

The prominent, bomb-rich units in the study area are inferred to have accumulated close to source vents undergoing Hawaiian and Strombolian eruptions, with some phreatomagmatic input at times. Eruptive episodes alternated with periods of quiet lacustrine sedimentation during ongoing subsidence, presumably within an intra-arc basin. Bomb sags are present in all cases where the deposits rest directly on lacustrine strata (Fig. 10), which must have been unlithified and moist (cohesive) when the bombs impacted. However, the pyroclasts show no evidence of rapid aqueous chilling, which would be expected if they fell into lakes containing a significant amount of water. The lakes were probably shallow at any given time, so that rapid influx of coarse pyroclasts dominated the thermal regime and suppressed aqueous quenching.

Additional evidence that the lacustrine sediments were wet and unconsolidated during the volcanic activity is provided by development of peperite between intrusive magma and sediment, and by the presence of partly disaggregated sediment masses contained within the intrusive pyroclastic rocks. Intercalation of massive bomb-rich units with generally fine-grained, unconsolidated sediments rich in pore water probably created a setting favorable for intrusive pyroclastic activity. A model for the development of the intrusive pyroclastic rocks is shown in Fig. 20, in which a postulated vent conduit feeding explosive pyroclastic eruptions at the surface is shown cutting across previously deposited pyroclastic and lacustrine units. We infer that, at times during the ongoing eruption, jets of intrusive pyroclastic material were blasted laterally from the conduit into layers of weak sediments forming parts of the conduit walls. This might have been triggered when collapse of parts of the ejecta rim or walls into the conduit at higher levels impeded upwards thrust of gas and pyroclasts from magmatic explosions originating deeper in the conduit. Several examples of the intrusive pyroclastic rock occur only a short distance below the massive, bomb-rich pyroclastic units (e.g., measured section M-3 in Fig. 4), suggesting that these units resisted penetration by the intrusive pyroclastic material, resulting in significant lateral motion of the pyroclastic jets into weak sediments between bomb-rich layers. Liquefaction and fluidization of the sediments as their pore water was converted to steam likely helped create space for the intrusive pyroclastic jets.

Zones of peperite must have formed after explosive activity ceased, when magma rising up in the conduit intruded along planes of weakness between still unconsolidated, water-rich sediment and intrusive pyroclastic material (Fig. 20), resulting in nonexplosive quenching and commingling of the magma with the wet sediment. Coherent hypabyssal intrusions in the area also were injected into unconsolidated material, as shown by the common presence of undulatory chilled margins along intrusive contacts (e.g., Keating et al., 2008; Befus et al., 2009) and by breakup of some intrusive tongues penetrating into the intrusive pyroclastic masses (Figs. 12 and 19).

Reports of intrusive pyroclastic rocks in the literature are relatively sparse, although several examples have been described of welded felsic ignimbrites filling vents that supplied explosive magmatic eruptions (Wolff, 1986; Reedman et al., 1987). Tuffisite injections in felsic and andesitic lava flows and domes appear to be common (e.g., Tuffen et al., 2003) but are developed on a much smaller scale. Dikes and sills filled with pyroclasts generated during subsurface phreatomagmatic explosions have also been reported (e.g., Hanson and Elliot, 1996). Reports of intrusive basaltic to andesitic pyroclastic rocks of the type described in the present poster, consisting of vesicular lapilli and bombs, are much less common. One well documented Miocene example in California consists of a complex of sills and dikes that extends laterally for ~10 km and formed when intrusive andesitic pyroclasts (pumice lapilli and ash) were injected into unlithified diatomite at very shallow levels beneath the seafloor (Schleicher, 1974).

It is possible that intrusive basaltic to andesitic pyroclastic rocks are more common than generally realized but have been overlooked because they closely resemble extrusive pyroclastic deposits produced by Hawaiian or Strombolian eruptions. Detailed studies in other volcanic terrains exposing hypabyssal magma plumbing systems to volcanoes of various types are likely to reveal other examples.

References

Befus, K.S., Hanson, R.E., Miggins, D.P., Breyer, J.A., and Busbey, A.B., 2009, Nonexplosive and explosive magma/wet-sediment interaction during emplacement of Eocene intrusions into Cretaceous to Eocene strata, Trans-Pecos igneous province, West Texas: Journal of Volcanology and Geothermal Research, v. 181, p. 155-172.
Brown, G.J., and Wilson, A.H., 1986, The petrology and geochemistry of the Barby Formation, Sinclair Sequence: Communications of the Geological Survey of Southwest Africa/Namibia, v. 2, p. 93-108.
Cornell, D.H., van Schijndel, V., Simonsen, S.L., and Frei, D., 2015, Geochronology of Mesoproterozoic hybrid intrusions in the Konkiep terrane, Namibia, from passive to active continental margin in the Namaqua-Natal Wilson cycle: Precambrian Research, v. 265, p. 166-188.
Cornell, D.H., Mapani, B., Malobela, T., Lundell, C., Harris, M., Jonsson, A., and Frei, D., 2016, Precise zircon dating identifies the threefold evolution of the Sinclair Supergroup of Namibia: Abstracts, 35th International Geological Congress, Cape Town, South Africa.
Hanson, R.E., 2003, Proterozoic geochronology and tectonic evolution of southern Africa, *in* Yoshida, M., Windley, B., and Dasgupta, S., eds., Proterozoic East Gondwana: Supercontinent Assembly and Breakup: Geological Society of London Special Publication 206, p. 428-463.
Hanson, R.E., and Elliot, D.H., 1996, Rift-related Jurassic basaltic phreatomagmatism in the central Transantarctic Mountains: precursory stage to flood-basalt volcanism: Bulletin of Volcanology, v. 58, p. 327-347.
Hoal, B.G., 1990, The geology and geochemistry of the Proterozoic Awasib Mountain Terrain, southern Namibia: Geological Survey of Namibia, Memoir 11, 163 p.
Hoal, B.G., 1993, The Proterozoic Sinclair Sequence in southern Namibia: intracratonic rift or active continental margin setting? Precambrian Research, v. 63, p. 143-162.
Jacobs, J., Pisarevsky, S., Thomas, R.J., and Becker, T., 2008, The Kalahari craton during the assembly and dispersal of Rodinia: Precambrian Research, v. 160, p. 142-158.
Keating, G.N., Valentine, G.A., Krier, D.J., and Perry, F.V., 2008, Shallow plumbing systems for small-volume basaltic volcanoes: Bulletin of Volcanology, v. 709, p. 563-582.
Miller, R.McG., 2008, The Geology of Namibia, Vol. 1, Archaean to Mesoproterozoic: Windhoek, Geological Survey of Namibia, p. 8-1 to 8-104.
Miller, R.McG., 2012, Review of Mesoproterozoic magmatism, sedimentation and terrane amalgamation in southwestern Africa: South African Journal of Geology, v. 115, p. 417-448.
Panzik, J.E., Evans, D.A.D., Kasbohm, J.J., Hanson, R., Gose, W., and DesOrmeau, J., 2016, Using palaeomagnetism to determine late Mesoproterozoic palaeogeographic history and tectonic relations of the Sinclair Terrane, Namaqua orogen, Namibia, *in* Li, Z.X., Evans, D.A.D., and Murphy, J.B., eds., Supercontinent Cycles through Earth History: Geological Society of London Special Publication 424, p. 119-143.
Reedman, A.J., Park, K.H., Merriman, R.J., and Kim, S.E., 1987, Welded tuff infilling a volcanic vent at Weolseong, Republic of Korea: Bulletin of Volcanology, v. 49, p. 541-546.
Schleicher, D., 1974, Emplacement mechanism of the Miraleste Tuff Bed, Palos Verdes Hills, California: Geological Society of America Bulletin, v. 85, p. 505-512.
Singletary, S.J., Hanson, R.E., Martin, M.W., Crowley, J.L., Bowring, S.A., Key, R.M., Ramokate, L.V., Direng, B.B., and Krol, M.A., 2003, Geochronology of basement rocks in the Kalahari Desert, Botswana, and implications for regional Proterozoic tectonics: Precambrian Research, v. 121, p. 47-71.
Tuffen, H., Dingwell, D.B., and Pinkerton, H., 2003, Repeated fracture and healing of silicic magma generate flow banding and earthquakes? Geology, v. 31, p. 1089-1992.
Watters, B.R., 1974, Stratigraphy, igneous petrology and evolution of the Sinclair Group in southern South West Africa: University of Cape Town, Precambrian Research Unit Bulletin 16, 235 p.
Wohletz, K.H., 1986, Explosive magma-water interactions: Thermodynamics, explosion mechanisms, and field studies: Bulletin of Volcanology, v. 48, p. 254-264.
Wolff, J.A., 1986, Welded-tuff dykes, conduit closure, and lava dome growth at the end of explosive eruptions: Journal of Volcanology and Geothermal Research, v. 28, p. 379-384.